Vol. 21, e210026 (2024)
doi: 10.2142/biophysico.bppb-v21.0026

Biophysics and Physicobiology
https://www.jstage.jst.go.jp/browse/biophysico/

Regular Article

Electrophysiological analysis of hyperkalemic cardiomyocytes using a multielectrode array system

Kentaro Kito, Masahito Hayashi, Tomoyuki Kaneko

Department of Frontier Bioscience, Graduate School of Science & Engineering, Hosei University, Koganei, Tokyo 184-8584, Japan

Received September 11, 2024; Accepted November 19, 2024;
Released online in J-STAGE as advance publication November 21, 2024
Edited by Haruki Nakamura

The action potential of cardiomyocytes is controlled by electrolytes in serum such as Na^+, K^+ and Ca^{2+}. Hyperkalemia, which refers to an abnormally high concentration of K^+ in the blood, can induce lethal arrythmia. In this study, the extracellular potentials on a sheet of chick embryonic cardiomyocytes were investigated at increasing K^+ concentrations using a multielectrode array system. We observed that the interspike interval (ISI) was prolonged by approximately 3.5 times; dV/dt (the slope of a waveform) was decreased by more than five times; the field potential duration (FPD) was shortened by 20%, and the conduction velocity was about half at 12 mM K^+ against the control (4 mM K^+). In calcium therapy for hyperkalemia, although the prolongation of ISI under hyperkalemic conditions was restored, the slowing of conduction velocity, the decrease in dV/dt, and the shortening of FPD were not recovered by increasing the extracellular Ca^{2+} concentration. These findings provide a comprehensive understanding of cardiomyocytes in hyperkalemic conditions. Electrophysiological analysis by varying the extracellular concentrations of multiple types of electrolytes will be useful for the further discussion of the results of this study and for the interpretation of the waveforms obtained by measuring the extracellular potential.

Key words: hyperkalemia, extracellular potential, calcium therapy

Significance

Hyperkalemia, which causes arrythmia, refers to an abnormally high K^+ level in the blood caused by renal failure. In this study, we perform electrophysiological analysis of hyperkalemic cardiomyocytes using a multielectrode array that can noninvasively measure the extracellular potential of cardiomyocytes. Consequently, our system reproduced the changes of the patch-clamp method or electrocardiogram (ECG) under hyperkalemic conditions. Compared with the patch-clamp method or ECG, our system could perform noninvasive and convenient analysis. These findings provide comprehensive understanding of cardiomyocytes in hyperkalemic conditions.

Introduction

The beating of the heart is controlled by electrolytes in serum such as Na^+, K^+ and Ca^{2+}. An imbalance among these ions causes arrhythmia. The concentration of K^+ is normally maintained between 4.0 and 4.5 mM in the human body. Hyperkalemia is a clinical condition that can induce lethal arrhythmia. This condition is due to the failure to excrete excess K^+ with decreased renal function. The European Resuscitation Council defines hyperkalemia as extracellular K^+ concentration of >5.5 mM, and severe hyperkalemia is defined as an extracellular K^+ concentration of >6.5 mM [1]. As

Corresponding author: Tomoyuki Kaneko, Department of Frontier Bioscience, Graduate School of Science & Engineering, Hosei University, 3-7-2 Kajino-cho, Koganei, Tokyo 184-8584, Japan. ORCID iD: https://orcid.org/0009-0009-6494-4418, e-mail: tkaneko@hosei.ac.jp

the concentration of K^+ increases, the resting membrane potential of cardiomyocytes increases, and changes appear on the electrocardiogram (ECG) [2,3]. For example, characteristic changes occur, such as the widening of the QRS interval and the appearance of tent-shaped T waves on the ECG [3]. There are three main treatments for hyperkalemia. First, increasing the concentration of extracellular Ca^{2+} can increase the threshold potential for depolarization and the maximum upstroke velocity (V_{max}) of the action potential. Ca^{2+} antagonizes the effects of hyperkalemia [2]. Second, a cation exchange resin can be administered to a patient to remove excess K^+ [2]. Third, insulin or glucose can be administered to the bloodstream to promote the uptake of K^+ into cells [2,4,5]. Performing electrophysiological analysis for cultured cardiomyocytes that simulated a hyperkalemic state is important because hyperkalemia is a potentially fatal arrythmia.

In general, the action potential of the cardiomyocytes was measured using a patch-clamp. This method uses a micropipette to attach to the ion channel of a single cell and measures the current using a microelectrode [6,7]. However, in this method, long-term measurement is difficult, and conduction analysis cannot be performed because it measures a single cell. This method also requires highly skilled and experienced operators. Thus, fluorescence imaging methods using membrane potential-sensitive fluorescent dyes have been used for conduction analysis of cardiomyocytes [8-10]. Long-term measurements are difficult to perform because of the cytotoxicity of excitation light and fluorescent dyes. By contrast, multielectrode array (MEA) system enables noninvasive long-term measurement of the extracellular potential [11], and it is more user friendly than the patch-clamp. This system can measure the extracellular potential of cardiomyocytes and neurons attached to 64 electrodes. It can also perform conduction analysis of cardiomyocytes by simultaneously measuring multiple electrodes [12,13]. The MEA system has attracted considerable attention from many pharmaceutical companies as an alternative to the patch-clamp method that has traditionally been the mainstream in non-clinical studies because of its noninvasiveness and its ability to simultaneously measure multiple electrodes. Research has been conducted on the development of a cardiotoxicity testing method using human embryonic stem cell and human induced pluripotent stem cell-derived cardiomyocytes with the MEA system [11–13].

In this study, the stepwise increase of the K^+ concentration in a culture medium for the treatment of hyperkalemia and the stepwise increase of the Ca^{2+} concentration in a culture medium under hyperkalemic conditions for the treatment of 7-day-old chick embryonic cardiomyocytes were investigated. The extracellular potential was also measured using the MEA system to investigate the effects of increased extracellular K^+ concentration on cardiomyocyte activity. In addition, the interspike interval (ISI), which indicates the beat interval, conduction velocity, and dV/dt of the waveform, was calculated. Furthermore, the effects of hyperkalemic cardiomyocyte activity and the electrophysiological effects of calcium therapy on hyperkalemia were evaluated.

Materials and Methods

Isolation of Cardiomyocytes from Chick Embryos

Cardiomyocytes were isolated from a 7-day-old chick embryonic heart by modifying a previously described method [14,15]. In brief, chicken eggs (Yamagishi, fertilized egg for research) were placed in an incubator (38°C, 60% humidity) for 7 days. The hearts were removed from embryonic chicks and transferred to D-MEM/Ham's F-12 with L-glutamine and Phenol Red (Wako, 048-29785) supplemented with 10% fetal bovine serum (Biosera, FB-1290/500), 100 units/mL penicillin and 100 μg/mL streptomycin (Wako, 168-23191) (abbreviated as DMEM). Subsequently, the hearts were minced into 1-mm^3 pieces to obtain cardiac tissues. The tissues were washed with PBS (−) (137 mM NaCl, 2.68 mM KCl, 10 mM $Na_2HPO_4 \cdot 12H_2O$, and 2 mM KH_2PO_4) and incubated at 37°C for 10 min in 10 mL of PBS (−) containing 0.1% collagenase (Sigma Aldrich, CO130-100MG) to suspend the coronary artery cells. Afterward, this supernatant liquid was discarded and incubated at 37°C for 20 min in 10 mL of PBS (−) containing 0.1% collagenase to digest the cardiac tissue. The cell suspension was filtered through a 100-μm nylon cell strainer (FALCON, 352360) and centrifuged at 195 g for 5 min at 20°C. The pellet, including the cardiac cells, was resuspended in DMEM. The suspension was placed on a 75-cm^2 tissue culture dish and incubated at 37°C and 5% CO_2 for 20 min to increase the purity of the cardiomyocytes by adhering to the fibroblasts.

Culture of Chick Embryonic Cardiomyocytes on the MEA Chip

The surface of the MEA chip (Alpha MED Scientific Inc., MED-R545A; Fig. 1A) was hydrophilized using a plasma device (Yamato Scientific, PM100) and coated with collagen type I-C (Nitta Gelatin, 130607). The isolated cardiomyocyte suspension (2.0×10^7 cells/mL, 40 μL) was dispersed on the MEA chip and incubated at 37°C and 5% CO_2. The DMEM in the MEA chip was replaced with fresh DMEM every day.

Extracellular Potential Recording Using the MEA System

Extracellular potential recording of cardiomyocytes was performed using the MEA system (Yasuda Lab., Waseda University, Japan) at a sampling rate of 10 kHz with a low path filter of 2 kHz and a high path filter of 1 Hz. The recording was amplified by 100–50,000 using an amplifier. All measurements were performed at 37°C. The concentration of K^+

was stepwise increased from 4 mM to 6, 8, 10, and 12 mM (DMEM contains 4 mM K^+) and washed out three times with fresh DMEM. These changes in K^+ concentration were made by replacing the entire DMEM. The concentration of Ca^{2+} was stepwise increased to 2, 3, 4, and 5 mM in DMEM under hyperkalemic conditions (12 mM K^+, 1 mM Ca^{2+}). MEA measurement was started immediately after replacing each solution, and the measurement data were saved to a hard disk drive.

Data Analysis

In analyzing the extracellular potential of the cardiomyocyte sheet acquired using the MEA chip (Fig. 1A), homemade codes written in Python3 (https://github.com/kkito0726/MEA_modules) were used, which calculate the ISI as an indicator of the beating intervals and the field potential duration (FPD) as an indicator of the QT interval on the ECG (Figs. 1B and C). The conduction velocity of the electrical waves on the cardiomyocyte sheet was calculated in accordance with the velocity mapping method of Dou *et al.* [16]. First, the arrival time of a conduction wave at each MEA electrode was obtained as the timepoint when its negative peak was observed (Fig. 1E). Second, a set of arrival times at 64 MEA electrodes, $t(x, y)$, was fitted to a third-order polynomial surface using the following equation:

$$t(x,y) = p_{00} + p_{10}x + p_{01}y + p_{20}x^2 + p_{11}xy + p_{02}y^2 + p_{30}x^3 + p_{21}x^2y + p_{12}xy^2 + p_{03}y^3 \ , \quad (1)$$

where p_{ij} is the fitting parameter of the surface. Third, $\nabla t(x, y)$, which is the gradient of $t(x, y)$, is calculated as follows:

$$\nabla t_x = p_{10} + 2p_{20}x + p_{11}y + 3p_{30}x^2 + 2p_{21}xy + p_{12}y^2,$$
$$\nabla t_y = p_{01} + p_{11}x + 2p_{02}y + p_{21}x^2 + 2p_{12}xy + 3p_{03}y^2. \quad (2)$$

The velocity vector of the conducting wave, $\boldsymbol{v}(x, y)$, is the product of the absolute velocity, $1/|\nabla t(x, y)|$. In addition, the unit vector of $\nabla t(x, y)$ is calculated as follows (Fig. 1D):

$$\boldsymbol{v}(x,y) = \left[\frac{\nabla t_x}{\nabla t_x{}^2+\nabla t_y{}^2}, \frac{\nabla t_y}{\nabla t_x{}^2+\nabla t_y{}^2}\right]. \quad (3)$$

Cardiomyocytes were isolated from a 7-day-old chick embryo heart to measure the extracellular potential of chick embryonic cardiomyocytes. These cardiomyocytes seed on the MEA chip (Fig. 1A). One day after cell seeding (Day 1), synchronized cardiomyocyte sheets were formed. On Day 3, the ISI (Fig. 1C) of the cardiomyocyte sheet was stable, and the conduction velocity reached its maximum velocity and stable. A conduction map was created using the negative peak time of each electrode as the conduction arrival time, and the conduction velocity was calculated from there (Fig. 1D). The slope of the waveform (dV/dt) was calculated using the potential difference and time difference between the positive and negative peaks (Fig. 1E).

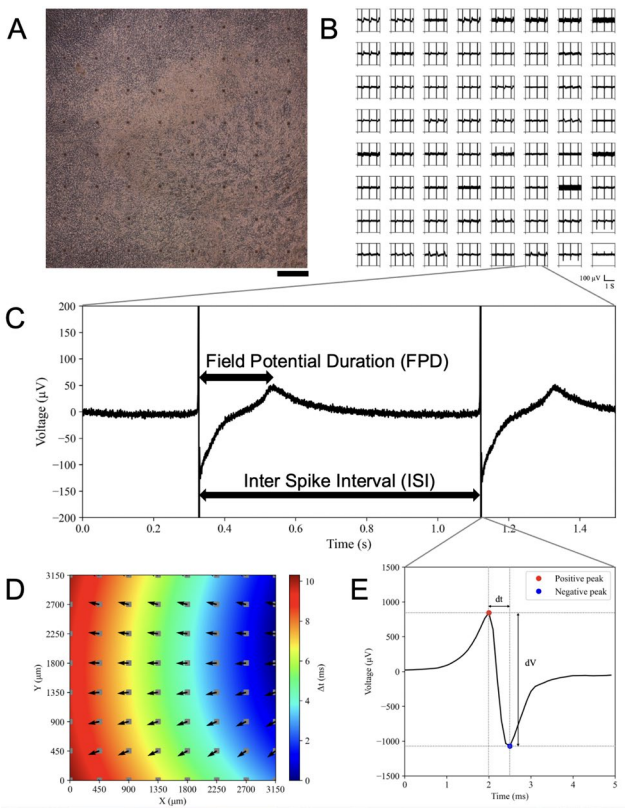

Figure 1 Extracellular potential recording using the MEA system and data analysis. (A) A phase contrast image of chick embryonic cardiomyocytes. Scale bar indicates 450 μm. (B) Waveforms detected by 64 electrodes. The arrangement of the graph matches the electrode arrangement. (C) The inter spike interval (ISI) is defined as the interval between the negative peaks, which indicates the beating interval. The field potential duration (FPD) is defined as the interval between the negative peak and the small positive peak after the negative peak. (D) Conduction map of cardiomyocytes. The length and direction of each black arrow indicate the conduction velocity and direction, respectively. Gray squares indicate the position of the electrode. (E) The difference between voltage and time between the positive and negative peaks is indicated as dV and dt, respectively, which is calculated as dV/dt.

Results

In evaluating the effects of increased extracellular K^+ concentration on cardiomyocytes, the culture media in the MEA chip were changed at the stepwise increase of the K^+ concentration in DMEM and washed with fresh DMEM. The ISI, conduction velocity, dV/dt, and FPD were calculated from the waveforms of the field potentials of the cardiomyocytes. ISI was prolonged with the increase of K^+ concentration. It was 3.5 times longer at 12 mM K^+ than at 4 mM (Fig. 2A). The conduction velocity decreased with the increase of K^+ concentration, with a significant decrease at 8 mM K^+. The conduction velocity further decreased to about half at 12 mM K^+ (Fig. 2B). Typical waveforms at each concentration were overlaid to evaluate the shape of the waveform (Fig. 2C). The waveform appeared to be disordered as the concentration of K^+ increased. Moreover, dV/dt decreased with the increase of K^+ concentration, with a significant decrease at 8 mM K^+ and a decrease of more than five times at 12 mM K^+ (Fig. 2D). These changes were recovered by washing out with fresh DMEM. Therefore, such changes are reversible. Typical waveforms around the second peak at each concentration were overlaid to evaluate the changes in FPD (Fig. 2E). The FPD on representative waves was calculated (Supplementary Fig. S1 (A)), and other waves (Supplementary Fig. S1 (B)) were excluded from the FPD calculation. The second peaks moved to the left and increased in size with the increase of K^+ concentration. The FPD was shortened by approximately 25% with the increase of K^+ concentration (Fig. 2F).

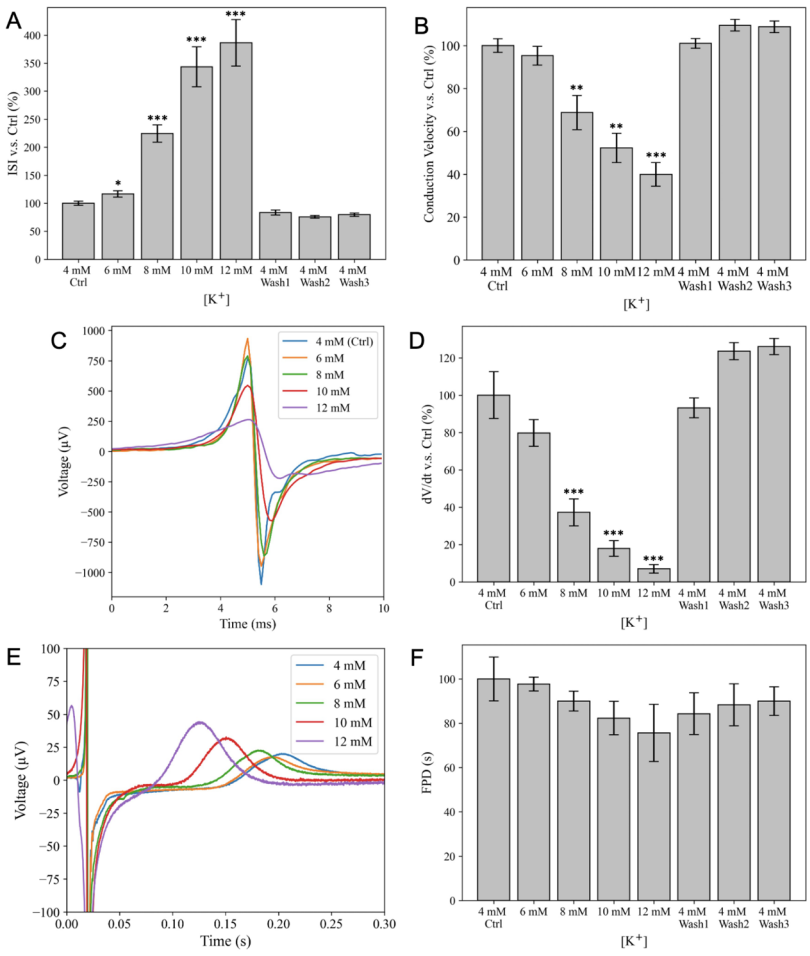

Figure 2 Changes in ISI, conduction velocity, dV/dt, and FPD with increasing of K^+ concentration. (A) Prolongation of ISI with the increase of K^+ concentration (mean ± SE, n = 11). (B) Slowing of conduction velocity with the increase of K^+ concentration (mean ± SE, n = 10). (C) Waveforms at each concentration. (D) Changes in dV/dt with the increase of K^+ concentration (mean ± SE, n = 11). (E) Average waveforms at each concentration. (F) Shortened FPD with the increase of K^+ concentration (mean ± SD, n = 45). Data were expressed as $*p < 0.03$, $**p < 0.01$, and $***p < 10^{-4}$; t-test versus control.

In evaluating the relationship between dV/dt and the conduction velocity on each electrode, we recalculated the conduction velocity at the electrodes for which dV/dt could be calculated. Then, dV/dt and the conduction velocity were replotted on the X-axis and Y-axis, respectively (Fig. 3). The relationships between the other parameters are shown in Supplementary Figure S2. The conduction velocity increased with the increase of dV/dt, and the rate of change gradually decreased. The change was fitted to the logarithmic function.

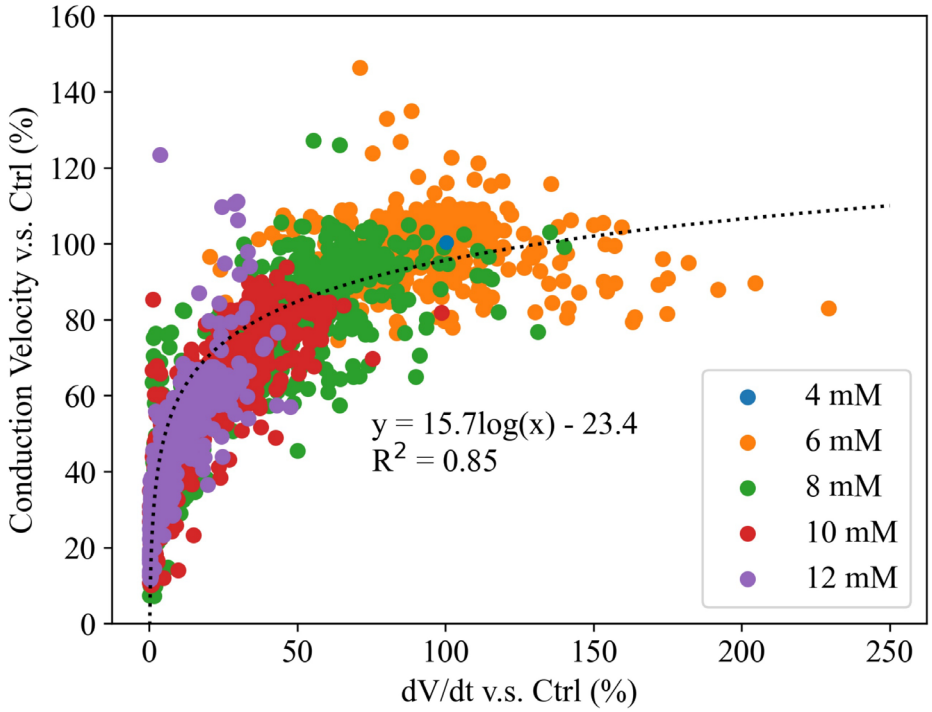

Figure 3 Relationship between dV/dt and the conduction velocity. The circles with different colors indicate the concentration of K^+. n = 10.

Furthermore, the effect of calcium therapy for hyperkalemia on a cardiomyocyte sheet was investigated. The prolongation of ISI under hyperkalemic conditions was restored with each increase in Ca^{2+} concentration (Fig. 4A). However, the slowing of conduction velocity (Fig. 4B), the decrease in dV/dt (Fig. 4C), and the shortening of FPD (Fig. 4D) were not recovered by increasing the extracellular Ca^{2+} concentration.

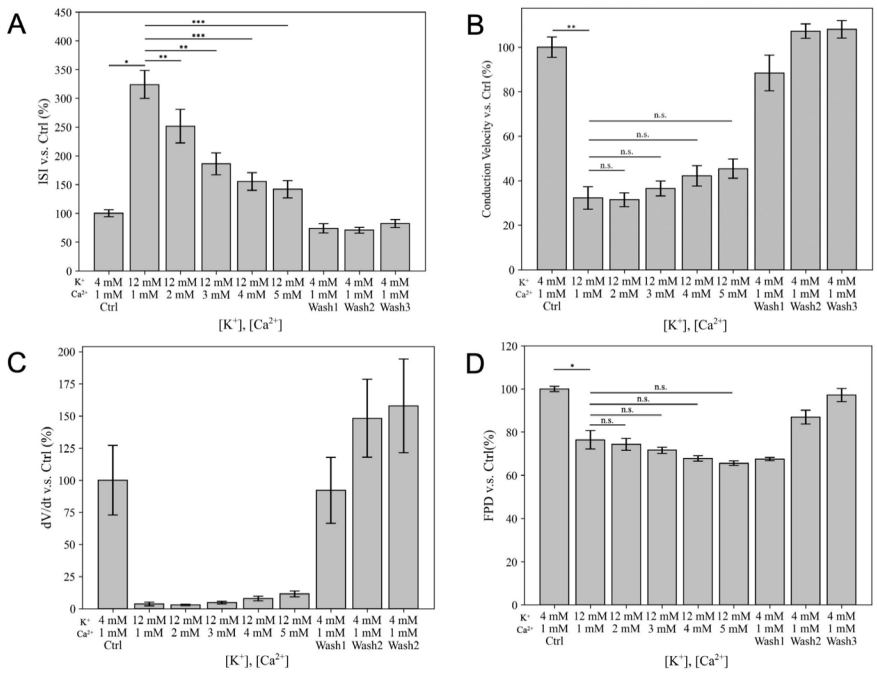

Figure 4 Changes in ISI, conduction velocity, dV/dt, and FPD during calcium therapy for hyperkalemia. Changes in (A) ISI, (B) conduction velocity, (C) dV/dt, and (D) FPD with the increase of Ca^{2+} concentration under hyperkalemic conditions. All data were expressed as mean ± SE, $*p < 0.03$, $**p < 0.01$, and $***p < 10^{-4}$; t-test, n = 5.

Discussion

In clinical practice, severe hyperkalemia is diagnosed when the blood K^+ concentration exceeds 6.5 mM [1] and shows symptoms of bradyarrhythmia with ECG changes in human hearts. In this study, the ISI showed significant prolongation at 6 mM K^+ (Fig. 2A) in chick embryonic cardiomyocytes. This response corresponds to bradyarrhythmia induced by hyperkalemia. The FPD was also shortened by approximately 30%, which corresponds to QT interval shortening due to hyperkalemia (Fig. 2F).

A slowing of the conduction velocity and a decrease in dV/dt were also observed in the cardiomyocytes with the increase of K^+ concentration (Fig. 3). This delay in conduction velocity may be due to a decrease in the excitation rate of cardiomyocytes caused by a decrease in the activated sodium ion channels and a decrease in the resting membrane potential. In a previous study, the resting membrane potential of cardiomyocytes decreased from −90 mV to −70 mV under hyperkalemic conditions [2,17]. Therefore, using the patch-clamp method, the number of available sodium ion channels decreases, and the rate of phase 0 increase of the action potential (V_{max}) decreases [2,17]. In tissue slices, increasing K^+ to 12 mM reduced V_{max} to about 27% of the control in the ventricular epicardium [17]. By contrast, in this study, dV/dt decreased more than 20% at 12 mM K^+ (Fig. 2D), indicating a similar tendency. The waveform obtained from measuring the extracellular potential in this study displayed a gradual slope under high K^+ concentration. Therefore, the V_{max} of the action potential and the dV/dt of the extracellular potential are similar indicators. A decrease in the V_{max} of the action potential indicates that the excitation rate of cardiomyocytes decreases. This delay in velocity affects the conduction velocity to the neighboring cardiomyocyte, which explains the slowing of the conduction velocity observed in this study.

In the treatment of hyperkalemia, three main methods are known in clinical practice. First, Ca^{2+} is often administered into the blood because it antagonizes the effect of high K^+ concentration [2]. Calcium therapy is known for its membrane-stabilizing effects, typically on the normalization of resting membrane potential [2,18–20]. Unlike the ISI, the conduction velocity, dV/dt, and FPD were not recovered with the increase of Ca^{2+} concentration in this study (Fig. 4). This result indicates that calcium therapy of the human heart only restores the beating pace of the heart. Second, a cation exchange resin (sodium polystyrene sulfonate, patiromer, etc.) can be administered into the gastrointestinal tract to adsorb K^+ and induce defecation, thereby returning blood K^+ levels to normal [2]. We reproduced the reduction of blood K^+ concentration in resin therapy by replacing the culture medium in the MEA chip in which cardiomyocytes were cultured with normal K^+ concentration. Third, insulin therapy reduces blood K^+ concentration by allowing the liver and other organs to absorb K^+ in concert with glucose absorption through the administration of insulin [2,4,5]. In this study, cardiomyocytes were only used in the experimental system, and the mechanism underlying K^+ absorption in hepatocytes was not reproduced. The effect of blood K^+ reduction in insulin therapy was reproduced by replacing the culture medium in the MEA chip. In the future, combining a medium exchange procedure that mimics the temporal changes in blood K^+ associated with resin and insulin therapy in clinical practice will contribute to the elucidation of the mechanism underlying cardiomyocyte pulsatile recovery in response to changes in patient conditions.

In our test model, the K^+ concentrations cover a wide range and exceed those typically observed in clinical hyperkalemia. Although this K^+ concentration is an advantage of the *in vitro* system, it may not accurately reflect the responses observed in clinical *in vivo* conditions. This study did not mimic the structure of the heart, and the species were different. Thus, the response concentrations were different from the clinical conditions. In addition, given that the sensitivity to environmental changes can vary depending on the size and cell density of the cell population, cell culture conditions that reflect clinical conditions should be considered in future research. Furthermore, several cardiotoxicity tests have been performed using MEA systems with human ES or iPS cell-derived cardiomyocytes [11–13,21]. Although the waveform on the MEA system obtained by chick embryonic cardiomyocytes is similar to that of human stem cell-derived cardiomyocytes, the types and responses of the ion channels might be different between chick embryos and humans. Although the response of chick embryonic cardiomyocytes to changes in ion concentrations and drugs might be different from that to humans, the response of our test model to changes in K^+ concentration in this study was the same as that of human cardiomyocytes. This experiment confirms that the response of chick embryonic cardiomyocytes to changes in K^+ concentration is similar to that of humans. This finding may help to explain the utility of cardiotoxicity testing using chick embryonic cardiomyocytes.

Conclusion

Our system reproduced *in vitro* bradyarrhythmia and ECG changes such as increased QRS width and shortened QT that occur clinically during hyperkalemia. Bradycardia could be detected as ISI prolongation occurred, and ECG changes such as increase in QRS width with the decrease in dV/dt and QT shortening such as FPD shortening with the increase in concentration of K^+ were noted. Furthermore, conduction delays in the heart were detected as the slowing of conduction velocity. In addition, the benefit of calcium therapy during hyperkalemia was limited to a decrease in the beating rate and

was not significant for other indicators. Apart from hyperkalemia, various electrolyte disorders could be reproduced using the on-chip model system developed in this study, which might promote the development of new treatment methods.

Conflict of Interest

The authors declare no conflicts of interest.

Author Contributions

K.K., M.H. and T.K. designed the project. K.K. performed the experiments and analyzed the data. K.K., M.H. and T.K. wrote and checked the manuscript.

Data Availability

The evidence data generated and/or analyzed during the current study are available from the corresponding author on reasonable request.

Acknowledgements

We gratefully acknowledge the technical support of the Yasuda Laboratory, Waseda University, for the MEA system.

References

[1] Lott, C., Truhlář, A., Alfonzo, A., Barelli, A., González-Salvado, V., Hinkelbein, J., et al. European resuscitation council guidelines 2021: Cardiac arrest in special circumstances. Resuscitation 161, 152-219 (2021). https://doi.org/10.1016/j.resuscitation.2021.02.011

[2] Parham, W. A., Mehdirad, A. A., Biermann, K. M., Fredman, C. S. Hyperkalemia revisited. Tex. Heart Inst. J. 33, 40-47 (2006).

[3] Dittrich, K. L., Walls, R. M. Hyperkalemia: ECG manifestations and clinical considerations. J. Emerg. Med. 4, 449-455 (1986). https://doi.org/10.1016/0736-4679(86)90174-5

[4] Allon, M., Copkney, C. Albuterol and insulin for treatment of hyperkalemia in hemodialysis patients. Kidney Int. 38, 869-872 (1990). https://doi.org/10.1038/ki.1990.284

[5] Blumberg, A., Weidmann, P., Shaw, S., Gnädinger, M. Effect of various therapeutic approaches on plasma potassium and major regulating factors in terminal renal failure. Am. J. Med. 85, 507-512 (1988). https://doi.org/10.1016/S0002-9343(88)80086-X

[6] Sakmann, B., Neher, E. Patch clamp techniques for studying ionic channels in excitable membranes. Annu. Rev. Physiol. 46, 455-472 (1984). https://doi.org/10.1146/annurev.ph.46.030184.002323

[7] Kornreich, B. G. The patch clamp technique: principles and technical considerations. J. Vet. Cardiol. 9, 25-37 (2007). https://doi.org/10.1016/j.jvc.2007.02.001

[8] Fast, V. G. Simultaneous optical imaging of membrane potential and intracellular calcium. J. Electrocardiol. 38, 107-112 (2005). https://doi.org/10.1016/j.jelectrocard.2005.06.023

[9] McPheeters, M. T., Wang, Y. T., Werdich, A. A., Jenkins, M. W., Laurita, K. R. An infrared optical pacing system for screening cardiac electrophysiology in human cardiomyocytes. PLoS One 12, e0183761 (2017). https://doi.org/10.1371/journal.pone.0183761

[10] King, D. R., Entz, M. II, Blair, A. G., Crandell, I., Hanlon, L. A., Lin, J., et al. The conduction velocity-potassium relationship in the heart is modulated by sodium and calcium. Pflugers Arch. 473, 557-571 (2021). https://doi.org/10.1007/s00424-021-02537-y

[11] Kussauer, S., David, R., Lemcke, H. hiPSCs derived cardiac cells for drug and toxicity screening and disease modeling: What micro-electrode-array analyses can tell us. Cells 8, 1331 (2019). https://doi.org/10.3390/cells8111331

[12] Kaneko, T., Nomura, F., Hamada, T., Abe, Y., Takamori, H., Sakakura, T., et al. On-chip in vitro cell-network pre-clinical cardiac toxicity using spatiotemporal human cardiomyocyte measurement on a chip. Sci. Rep. 4, 4670 (2014). https://doi.org/10.1038/srep04670

[13] Asahi, Y., Hamada, T., Hattori, A., Matsuura, K., Odaka, M., Nomura, F., et al. On-chip spatiotemporal electrophysiological analysis of human stem cell derived cardiomyocytes enables quantitative assessment of proarrhythmia in drug development. Sci. Rep. 8, 14536 (2018). https://doi.org/10.1038/s41598-018-32921-1

[14] Kaneko, T., Toriumi, H., Shimada, J., Nomura, F. Extracellular field potential recording of single cardiomyocytes

in agarose microchambers using microelectrode array. Jpn. J. Appl. Phys. 57, 03EB03 (2018). https://doi.org/10.7567/JJAP.57.03EB03
[15] Fujii, K., Nomura, F., Kaneko, T. Dependences of the geometrical parameters of cell community on stimulation voltage and frequency in chick embryonic cardiomyocytes. Jpn. J. Appl. Phys. 57, 03EB04 (2018). https://doi.org/10.7567/JJAP.57.03EB04
[16] Dou, W., Zhao, Q., Malhi, M., Liu, X., Zhang, Z., Wang, L., et al. Label-free conduction velocity mapping and gap junction assessment of functional iPSC-Cardiomyocyte monolayers. Biosens. Bioelectron. 167, 112468 (2020). https://doi.org/10.1016/j.bios.2020.112468
[17] Cordeiro, J. M., Mazza, M., Goodrow, R., Ulahannan, N., Antzelevitch, C., Di Diego, J. M. Functionally distinct sodium channels in ventricular epicardial and endocardial cells contribute to a greater sensitivity of the epicardium to electrical depression. Am. J. Physiol. Heart Circ. Physiol. 295, H154-H162 (2008). https://doi.org/10.1152/ajpheart.01327.2007
[18] Weisberg, L. S. Management of severe hyperkalemia. Crit. Care Med. 36, 3246–3251 (2008). https://doi.org/10.1097/CCM.0b013e31818f222b
[19] Depret, F., Peacock, W. F., Liu, K. D., Rafique, Z., Rossignol, P., Legrand, M. Management of hyperkalemia in the acutely ill patient. Ann. Intensive Care 9, 32 (2019). https://doi.org/10.1186/s13613-019-0509-8
[20] Lindner, G., Burdmann, E. A., Clase, C. M., Hemmelgarn, B. R., Herzog, C. A., Małyszko, J., et al. Acute hyperkalemia in the emergency department: A summary from a kidney disease: Improving global outcomes conference. Eur. J. Emerg. Med. 27, 329-337 (2020). https://doi.org/10.1097/MEJ.0000000000000691
[21] Tanaka, T., Tohyama, S., Murata, M., Nomura, F., Kaneko, T., Chen, H., et al. In vitro pharmacologic testing using human induced pluripotent stem cell-derived cardiomyocytes. Biochem. Biophys. Res. Commun. 385, 497-502 (2009). https://doi.org/10.1016/j.bbrc.2009.05.073